Letters

A Novel Detachable Gate Driver Unit With Ultralow Inductance for Integrated Gate Commutated Thyristor

Jie Shang, Zhengyu Chen, Biao Zhao, *Senior Member, IEEE*, Zhanqing Yu, *Member, IEEE*, Jinpeng Wu, Lin Dong, and Rong Zeng, *Senior Member, IEEE*

***Abstract*—Under the background of clean energy connected to the grid, the high-capacity power electronics device integrated gate commutated thyristor (IGCT) has a bright future. In order to increase the convenience of replacement and longevity of service, a novel detachable gate driver unit (DGDU) concept for IGCT is proposed in this letter. To ensure the turn-OFF capability, both connection scheme and board optimization on DGDU are applied to minimize the stray inductance. Besides, the effects because of the detachable connecter on the structure and thermal characteristics are analyzed. Afterward, an overlapping scheme of DGDU with ultralow inductance is proposed for IGCT. Finally, a 4-inch prototype and a single-phase full-bridge platform are developed for the test. The turn-OFF capability of DGDU is verified by pulse experiment, which could turn-OFF a 5 kA current successfully. The stray inductance of DGDU is calculated based on the experimental result and is only 4% larger than conventional GDU, which means the commutation capability has little decrease. Furthermore, the continuous running reliability is verified by 2200 V-dc-voltage, 1300 A-effective-current power cycling experiments.**

***Index Terms*—Gate driver unit (GDU), integrated gate commutated thyristor (IGCT), power electronics, ultralow inductance.**

I. Introduction

With a large number of clean energy sources, such as wind power, connected to the power grid by power electronic converters, the high-capacity current-controlled device integrated gate commutated thyristor (IGCT) becomes one of the best options [1]. Existing commercial IGCTs have already achieved power levels above 4500 V/5000 A, and all the gate drive units (GDUs) are integrated with the GCT housing directly [2]. This close integration cannot only minimize the stray inductances in the gate-contact circuit, allowing for very high di/dt, but also swiftly commutates the anode current to the gate in 1us during the turn-OFF process to satisfy the "hard-drive limit" [3], which is the most important factor to increasing the maximum turn-OFF current of IGCT.

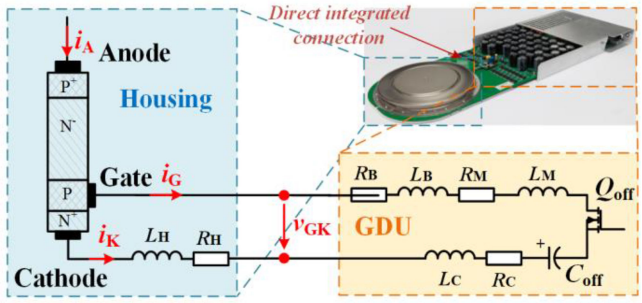

Fig. 1. Turn-OFF circuit of IGCT with parasitic parameters.

Fig. 1 shows the turn-OFF circuit of the IGCT with parasitic parameters. The turn-OFF MOSFET Q_{OFF} and the turn-OFF capacitor C_{OFF} are the major elements for current commutation. R_B, R_C, R_M, and R_H are the stray resistances of the PCB, capacitor, MOSFET, and GCT housing. Correspondingly, L_B, L_C, L_M, and L_H are the stray inductance of those parts, whose sum equals the total stray inductance L_S. When IGCT is turned-OFF, Q_{OFF} switches and the cathode current i_K are commutated toward the gate path forced by the precharged C_{OFF} (usually 20 V) [4]. The time of total anode current i_A commutated to gate (commutation time T_C) should be shorter than 1us (delay time T_D), during which the anode–cathode voltage v_{AK} begins to rise and then i_A reduces rapidly. If $T_C > T_D$, GCT could not turn OFF normally and would lead to thermal breakdown eventually. Thus, the complete driver board is chosen in order to reduce L_S, shorten T_C, and increase the turn-OFF capability ultimately. Specifically, the stray inductance L_S must be as low as 1–3 nH to commutate 5–10 kA current [5].

Conventional press-pack IGCTs are usually fastened in a series with 40–100 kN of pressure after integrating the GDU

Manuscript received 18 April 2022; revised 29 May 2022; accepted 25 June 2022. Date of publication 7 July 2022; date of current version 6 September 2022. This work was supported in part by the Key projects of the National Natural Science Foundation of China under Grant 51837006 and in part by the Integration projects of National Natural Science Foundation of China-State Grid Joint Fund for Smart Grid under Grant U1966602. *(Corresponding authors: Jinpeng Wu; Zhengyu Chen.)*

Jie Shang, Biao Zhao, Zhanqing Yu, Jinpeng Wu, and Rong Zeng are with the Department of Electrical Engineering, Tsinghua University, Beijing 100084, China (e-mail: shangj19@mails.tsinghua.edu.cn; zhaobiao112904829@126.com; yzq@tsinghua.edu.cn; wujinpengcn@gmail.com; zengrong@tsinghua.edu.cn).

Zhengyu Chen and Lin Dong are with DC Research Center, Sichuan Energy Internet Research Institute, Chengdu 610299, China (e-mail: chenzhen14@tsinghua.org.cn; donglin@tsinghua-eiri.org).

Color versions of one or more figures in this article are available at https://doi.org/10.1109/TPEL.2022.3187697.

Digital Object Identifier 10.1109/TPEL.2022.3187697

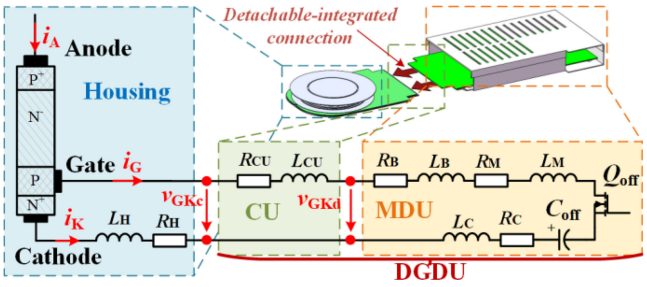

Fig. 2. Concept diagram of IGCT with DGDU and its parasitic parameters of turn-OFF circuit.

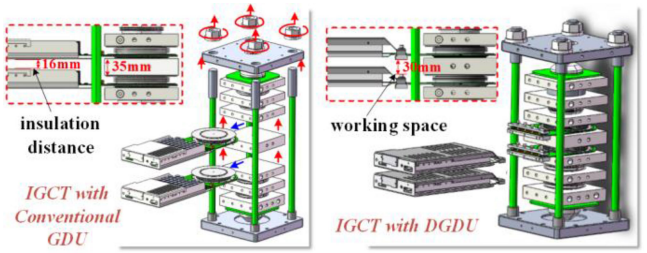

Fig. 3. Replacement of half-bridge valve series in converter.

with the housing. Frequent replacement and maintenance of IGCTs, especially GDUs, are necessary not only in experiments with valves but also during the overhaul, because of the shorter life span of GDUs than GCT wafers. Integrated GDUs would bring extra difficulty and cost for disassembly, especially on the narrow offshore platforms. Several concepts of gate turn-OFF thyristor detaching the GDU with the housing have been proposed, but a part of the driver circuit remained in or around the housing [6], [7], which prevents them from being used commercially.

Thus, a novel detachable gate driver concept is proposed for IGCT, and a design method based on overlap connection with ultralow inductance is provided in this letter.

II. Proposed DGDU Concept of IGCT

The concept diagram of IGCT with a detachable gate driver unit (DGDU) is shown in Fig. 2, consisting of the main driver unit and a connection unit. The highly reliable connection unit with no electronic components is integrated with GCT housing, which need not be replaced. The main driver unit containing lots of components is connected with the connection unit through a special interface structure with ultralow inductance, named as the detachable-integrated connection. Because of the detachable structure, a new term L_{CU} is added to the total inductance L_{S}, which represents the inductance of the connection unit and interface. Fig. 3 shows the replacement method for the two types of GDUs. For conventional GDU, the whole series must be disassembly, and then the complete IGCTs can be moved out. In comparison, the DGDU can be easily separated from the interface without disassembling the series. Furthermore, the added height of DGDU is very limited, and for a series with a 35 mm heat sink between IGCTs (to ensure the insulation distance between GDUs), the IGCT with two types of GDUs can be replaced directly without changing the series structure. A working space larger than 30 mm is reserved for assembling the main driver unit.

The detachable driver units of IGBT and thyristor have significant differences from IGCT. The IGBT only requires a negative voltage from the driver unit to cutoff the conductive channel. The thyristor cannot turn-OFF initiatively, so the driver unit only sends a 10–20 A of pulse current to trigger on the device. A wire of microhenry's inductance is enough for them.

For the detachable-integrated connection of DGDU, the inductance requirement is extremely rigorous. Only 20%–30% extra inductance (0.3 nH) is acceptable, which is three orders of magnitude lower than IGBT. Besides, the limited resistance and high structural strength requirement also must be considered.

III. Design of DGDU With Ultralow Inductance

A. Proposed Detachable Schemes With Ultralow Inductance

To achieve large current conduction capability and low stray inductance, a special scheme named bridge connection is proposed as Fig. 4(a) shown. The two boards are placed side by side, whose gate electrodes are both on the top layer and cathode on the bottom. The electrodes are connected by two busbars, respectively, like a bridge, which can increase the conduction capability. Additionally, the boards are six-layer PCBs, whose gate layers (orange, light color in the figure, on top, third, and fifth layer) and cathode layers (blue, dark color, on second, fourth, and bottom layer) are alternated for lower L_{S}. In addition, the large amount of via holes locates in the connection area to direct the current from the inner layers to the surface layers. Unfortunately, there is a gap between the two busbars, which might cause extra L_{S}. The busbars need to be welded or soldered to the connection unit, which is quite complicated.

Afterward, a compact overlap scheme [Fig. 4(b)] with ultralow inductance is proposed. The driver board and connecter board are overlapping, whose gate electrodes and cathode electrodes are in direct contact. The gate electrode of the driver board and the cathode electrode of the connecter board are located at the distal end, and the other electrodes are located inside. The PCB stackup and via holes are the same as the first scheme. This method not only has all advantages of the bridge method but also overcomes the gap between two boards, reduces the complexity, and achieves ultralow inductance.

B. Inductance Extraction and Analyses for Different Schemes

To obtain an accurate inductance result of different connection schemes of large and tight multilayer copper structures, three typical schemes are analyzed to find a tradeoff between the detachable method and turn-OFF capability

1) A: a 100 mm-length, six-layer board.
2) B: one 50 mm-length, and another 40 mm-length six-layer board bridge-connected by two copper busbars, whose total length are 100 mm.

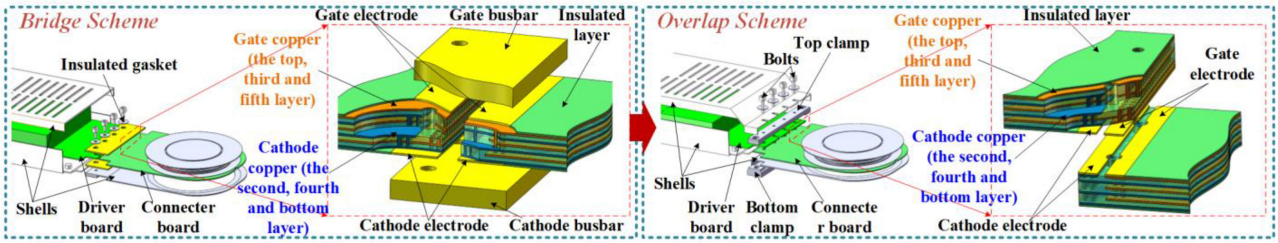

(a) (b)

Fig. 4. Proposed ultralow inductance design of connection schemes. (a) Bridge connection. (b) Overlap connection.

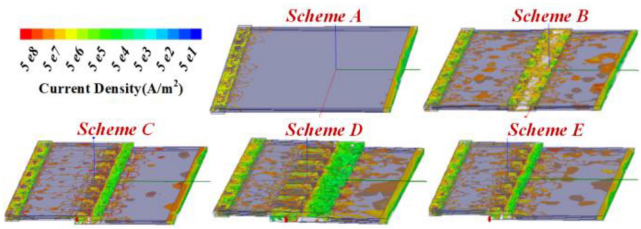

Fig. 5. Current density distribution with different schemes.

TABLE I
INDUCTANCE AT DIFFERENT FREQUENCIES

frequency /MHz	0.1	1	10	100	1000
Scheme A /pH	104.8	32.5	28.8	28.7	28.7
Scheme B /pH	356.1	322.3	320.7	320.6	320.6
Scheme C /pH	240.6	193.5	190.9	190.8	190.8
Scheme D /pH	293.0	225.9	222.6	222.4	222.4
Scheme E /pH	262.2	212.5	209.9	209.8	209.8

3) C: two 60 mm-length six-layer boards overlapped 20 mm, whose total length is 100 mm.

The A, B, and C are corresponding to the conventional GDU, bridge scheme, and overlap scheme, respectively. Only the inductance of PCB and connection interface is investigated, so the other parts of turn-OFF circuit are simplified to source and load blocks. Furthermore, the large amount of via holes conducting different layers is also simplified to several copper cuboids to reduce complexity, which hardly affects the current path. One-kA sinusoidal current is applied as excitation.

Fig. 5 shows that the current distributes uniformly within the boards but converges at the connectors and the load bars. The equivalent frequency during turn-OFF commutation (several kA/μs) is much larger than 100 MHz, at which frequency the inductance has already reached saturation (from Table I). The tens-picohenry's inductance of PCB (scheme A) only accounts for less than 5% of total commutation inductance. Relatively, the inductance of overlap PCBs is about six times that of the conventional single board, whereas that of bridge-connected PCBs is about eleven times, thus the overlap scheme is better.

C. Inductance Optimal and Design on Board for DGDU

Based on the overlap scheme, the length of the connecter area and the total length of the two boards also have effects on inductance. Two additional schemes are analyzed, corresponding to a longer connecter area, and longer total length compared with C:

1) D: two 70 mm-length six-layer boards overlapped 40 mm, whose total length is 100 mm.
2) E: one 60 mm-length, and another 80 mm-length six-layer board overlapped 20 mm, whose total length is 120 mm.

The results in Table I show that the length of both connecter and board should be shortened as much as possible. Considering the difficulty of manufacture and current-conducting capability, the optimal length of the connector is 20 mm.

In addition, other optimization could be applied to reduce L_S. For example, L_M could be reduced by changing the TO-package to no-leads QFN or Direct-FET packages; L_C could be reduced by paralleling a sufficient number of ceramic capacitors; and L_H could be reduced by optimizing the position of gate contact and segments on the wafer, as well as the housing structure.

IV. STRUCTURE AND THERMAL CHARACTERIZATION

Because the connecter changes the stress condition and thermal path of GDU, the following issues need to be analyzed: first, the reduction of mechanical strength because of split metal shells; second, the nonuniformity of contact resistance at the contact surface due to bolt fastening; and finally, the temperature rise caused by the heat loss of the stray resistance.

A. Mechanical Strength Characterization

To enhance the mechanical strength of the overlap connecter, aluminum alloy with excellent mechanical properties is used to design the total-covered shells and clamps. Fig. 6(a) shows the deformation of DGDU in applications, through which the maximum deformation quantity is about 1cm located at the distal end. This deformation differs little from that in the conventional GDU and is acceptable. In the simulation, the top and bottom faces of GCT were fixed, and other parts were subjected to standard earth gravity.

B. Contact Resistance Characterization

When the pressure is high enough, the contact resistance decreases almost no further and accounts for only a small

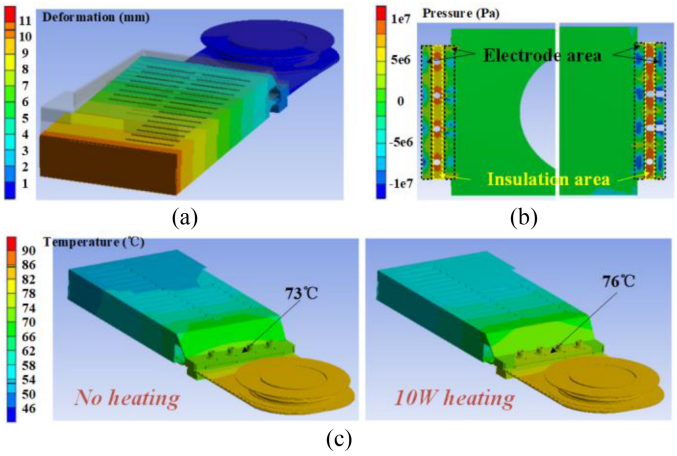

Fig. 6. Structure and thermal characterization. (a) Deformation of DGDU under earth gravity. (b) Pressure distribution on the two boards. (c) Temperature distribution with 10 W heating and no heating on contact resistance.

proportion of total resistance. To minimize the contact resistance of electrodes, the two boards are fastened by four steel bolts with 5000 N fastening force to each. Fig. 6(b) shows that the pressure in most of the electrode areas is within the range of 3–10 MPa, which is enough to ensure good contact and low resistance. However, this pressure is far less than the yield strength of PCB, so the PCB will almost never be irreversibly deformed or damaged. Thus, the conventional epoxy fiberglass fabric PCBs are used to control the cost. Besides, the contact resistance could be further reduced by changing the surface treatment process on electrodes. According to the experimental verification of the prototype, the contact resistance is less than 1 mΩ.

C. Temperature Rise Characterization

The DGDU might suffer extra heat loss generated by the 5–10 A turn-ON current and 5 kA turn-OFF commutation pulse, which are 10 W at most. Fortunately, voluminous metal shells and clamps sit snugly on the heated boards and act as a good radiator. Fig. 6(c) shows that the temperature deviation at the connecter is less than 3 °C with 10 W heating on the contact surface, and the deviation of minimum temperature on DGDU shells is less than 1.2 °C. The effect of such a low difference on drivers is negligible and is acceptable in applications. Considering the worst conditions, the simulation is under natural air convection heat dissipation, and the temperature of GCT housing is 85 °C and the ambient is 40 °C.

V. Prototype Implement and Experiment

A. Prototype Implementation

Based on the electromagnetic, thermal, and structural analysis above, it is proved that DGDU has excellent properties in all aspects. Afterward, a 4-inch prototype and a single-phase full-bridge platform have been developed and built to an experiment, as Fig. 7 shows. The overall length of the DGDU prototype is only 4% larger than that of the conventional GDU, whereas the width remains unchanged. Therefore, the conventional GDU can be substituted in most applications.

The experimental result of pressure distribution on the contact surface was measured by Fuji prescale. It can be seen that the pressure in most of the electrode areas is within the range of 6–10 MPa, which is even better distributed than expected.

B. Turn-off Capability

IGCT standard pulse test circuit was used to perform turn-OFF test on IGCT with DGDU and conventional GDU, using a 4.5 kV/5 kA 4-inch GCT device. The anode-cathode voltage v_{AK}, the gate-cathode voltage on driver board v_{GKd}, and on connecter board v_{GKc} were collected by voltage probes, and current i_{A}, i_{K} of IGCT were collected by Rogowski Coils.

Both two types of GDUs turned OFF 5 kA successfully as Fig. 8 shows. Focusing on v_{GK} in Fig. 8(b), the commutation time T_{C} of the two GDUs, which is equal to the times of transformation from $\mathrm{d}v_{\mathrm{GK}}/\mathrm{dt}>0$ to $\mathrm{d}v_{\mathrm{GK}}/\mathrm{dt}<0$, are both less than 700 ns, but the delay time T_{D} is larger than 900 ns. So the GCTs are both in the hard drive conditions. The proportion of stray inductance on each part of the turn-OFF circuit can be calculated based on the voltage distribution at the beginning of commutation when i_{G} is so small that the voltage on the stray resistance can be ignored (i.e., $L_{D1} : L_{D2} : L_{CU2} : L_H \approx 2 : 1 : 1.5 : 10$). Where, driver inductance L_{D} is the sum of L_{C}, L_{M}, and L_{B}; and subscript 1 and 2 represents conventional GDU and DGDU.

In conclusion, though the connecter brings additional stray inductance, the total inductance of GDGU is only 4% larger than that of conventional GDU, benefiting from the reduction of L_{D2} by optimization in components selection and PCB layout.

C. Power Cycling Experiment

The continuous operation capacity is verified by a power cycling experiment. By adjusting the phase angle difference of the inverter leg (T_1 and T_2) and rectifier leg (T_3 and T_4), the current on load inductor L_{load} can be adjusted to the set value. In the test, the voltage of C_{dc} was set to 2.2 kV, and the effective current of L_{load} was 1.3 kA under 14 ° phase angle difference. Several 2-h power cycles were carried out at different environment temperatures, and the waveform at 5 °C is as Fig. 8(c) shown. The turn-OFF peak current of IGCT was 1.8 kA, and the average switching frequency was 300 Hz. The temperature rise of GCT housing was about 20 °C when stabilized (with water cooling), and the overall temperature rise of the DGDU was less than 10 °C. Individual power chips reaching a 40 °C temperature rise are still limit. Besides, the pulse test result of all prototypes after power cycles performed the same as before.

Furthermore, some reliability tests, e.g., high-temperature test, rapid temperature transient test, vibration test, shock test, and salt spray test, have been systematic and comprehensive conducted, and all the DGDUs passed the tests. In particular, an accelerated aging experiment under 125 °C for a detachable interface has been conducted over 4 weeks and is still in progress, and few changes in the parasitic parameter and surface features have been found so far.

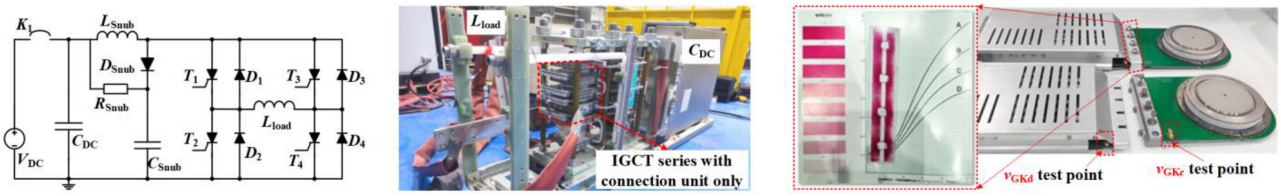

Fig. 7. Prototype implement and experiment platform. (a) Circuit of the single-phase full-bridge platform. (b) Photograph of the platform. (c) 4-inch prototype of DGDU for IGCT and the pressure experimental results on contact surface of driver and connecter board.

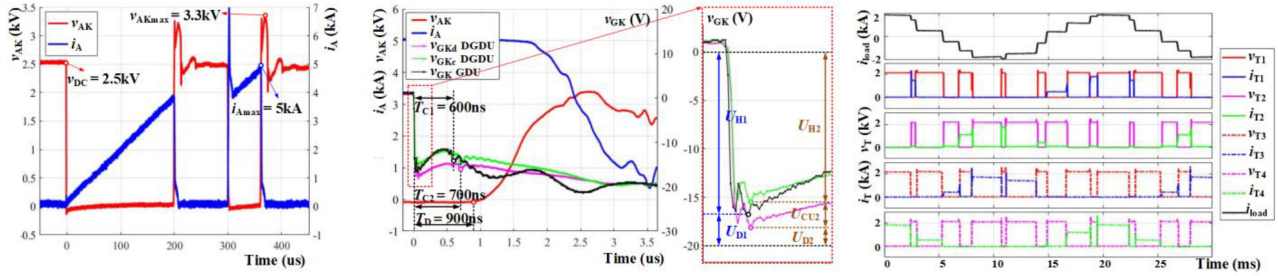

Fig. 8. Experiment waveform of DGDU. (a) Double-pulse test @2.5 kV/5 kA. (b) Detail contrast of the two GDUs. The v_{AK} and i_A are only given once because of the coincident waveform in two experiments. (c) Power cycling waveform at 5 °C temperatures.

VI. Conclusion

In this letter, the concept of DGDU and a typical design solution with ultralow inductance are proposed. The turn-OFF capability is verified by a pulse experiment with 4-inch prototype, which could turn-OFF 5 kA current successfully and is the same as conventional GDU. The stray inductance is only 4% increase. Therefore, the IGCT with DGDU is greatly convenient for disassembly, assembly and replacement, and has excellent prospects in the future field of high-power application.

References

[1] R. Zeng et al., "Integrated gate commutated thyristor-based modular multilevel converters: A promising solution for high-voltage dc applications," *IEEE Ind. Electron. Mag.*, vol. 13, no. 2, pp. 4–16, Jun. 2019, doi: 10.1109/MIE.2019.2906952.

[2] S. Bernet, "Recent developments of high power converters for industry and traction applications," *IEEE Trans. Power Electron.*, vol. 15, no. 6, pp. 1102–1117, Nov. 2000, doi: 10.1109/63.892825.

[3] I. Nistor, T. Wikstrom, and M. Scheinert, "IGCTs: High-power technology for power electronics applications," in *Proc. Int. Semicond. Conf.*, 2009, pp. 65–73, doi: 10.1109/SMICND.2009.5336607.

[4] Z. Chen et al., "An advanced 4-in integrated emitter Turn-off thyristor with ultralow commutation impedance to achieve 8 kA Turn-off capability: Comprehensive analysis, design, and experiments," *IEEE Trans. Ind. Electron.*, vol. 68, no. 10, pp. 9444–9454, Oct. 2021, doi: 10.1109/TIE.2020.3021645.

[5] Z. Chen, Z. Yu, X. Liu, J. Liu, and R. Zeng, "Stray impedance measurement and improvement of high-power IGCT gate driver units," *IEEE Trans. Power Electron.*, vol. 34, no. 7, pp. 6639–6647, Jul. 2019, doi: 10.1109/TPEL.2018.2826046.

[6] M. Bragard, C. Ronge, and R. W. De Doncker, "Sandwich design of high-power thyristor based devices with integrated MOSFET structure," in *Proc. 14th Eur. Conf. Power Electron. Appl.*, 2011, pp. 1–8.

[7] P. Koellensperger and R. W. D. Doncker, "The internally commutated thyristor - A new GCT with integrated turn-off unit," in *Proc. 4th Int. Conf. Integr. Power Syst.*, 2006, pp. 1–6.